2024 European Control Conference (ECC)
June 25-28, 2024. Stockholm, Sweden

Implementing EV Virtual Power Lines via Charging Station Control

Mladen Čičić, Carlos Canudas-de-Wit

***Abstract*— The impending green transition of the power system, brought about by the spread of Renewable Energy Sources, Energy Storage, and Electric Vehicles (EVs), calls for novel grid management solutions. Techniques using concepts such as Virtual Power Plants and Virtual Power Lines have already successfully been deployed to help manage the grid and shift power transmission in time. In this work, we propose and discuss a similar technique which can potentially match and surpass these results, which we refer to as EV Virtual Power Lines. By controlling the charging station prices and charging rates in a network in which EVs are circulating, we effectively shift the power consumption both in time and in space. This allows us to reinforce and balance the power grid, reducing grid congestion without disrupting EV operation. We model and analyse the dynamics of EVs circulating between two urban nodes in mixed traffic, and design control schemes that achieve charging station power reference tracking. Using a simple simulation example, performance achievable by applying such control schemes is demonstrated.**

I. Introduction

With the impending shift towards Renewable Energy Sources (RES) and Electric Vehicles (EVs), the demand for new approaches for active management of the power grid is progressively growing [1]. The distributed and intermittent nature of RES makes it challenging to model, analyse, and manage the impact that they have on the power grid. One way of dealing with this problem is to aggregate this generation into a single larger Virtual Power Plant [2], in an effort to reduce its variability. This technique also lends itself to utilization of latent energy storage and balancing resources of the charging EVs, as was done e.g., in the EDISON project [3]. Many similar approaches using smart EV charging, either to directly provide Active Network Management [4]–[6], or participate in the regulation market and provide ancillary services through vehicle-to-grid power transfer [7], [8], have been proposed in literature.

When discussing how EVs can help the power grid, there is a tendency to focus on the "E" (providing energy storage, as a battery), while neglecting the "V" (providing mobility, as a vehicle). These two aspects are often at odds, since an EV providing ancillary services at a charging station cannot be used for its primary role [9]. While in the case of privately owned EVs we may assume that they spend the majority of time parked, and that it is enough to charge them at home overnight [10], this is not the case for ride-hailing EVs, especially those with smaller batteries [11]. These EVs may be used throughout the day, need several recharges, and have little idle time when they can charge freely.

Mladen Čičić (cicic@berkeley.edu) is with Department of Civil and Environmental Engineering, University of California, Berkeley. Carlos Canudas-de-Wit (carlos.canudas-de-wit@gipsa-lab.fr) is with Univ. Grenoble Alpes, CNRS, Inria, Grenoble INP, and GIPSA-lab.

The main contribution of this work is in proposing a framework for controlling EV charging to reinforce the power grid through implementing an *EV Virtual Power Line* (EVPL), as outlined in Figure 1. Virtual Power Lines [12] are a proposed grid reinforcement technology that uses stationary energy storage to virtually transmit RES generation in excess of the grid capacity, by storing it and deferring transmission until the grid is no longer congested. In contrast to this approach, we propose using mobile distributed energy storage supplied by the circulating EVs. By providing incentives in the form of lower charging prices, we are able to influence these EVs' decisions on where to charge, effectively shifting power consumption from one location to another, without interrupting their operation. We study the model describing the dynamics of EV traffic and charging, and based on the analysis, design simple control laws using charging prices and charging rates as control inputs that achieve charging station power reference tracking and virtual power transmission.

In the rest of the paper, we first introduce the EVPL framework and outline its mechanism of action in Section II. Then, we present the model of mixed EV and non-EV traffic coupled with EV charging in Section III. Next, we propose control laws that achieve the desired EVPL power transmission in Section IV, which are then put to the test in simulations in Section V. Finally, in Section VI, we draw conclusions and outline directions for future work.

II. EV Virtual Power Lines

Consider the system outlined in Fig. 1, with two geographically distant urban nodes connected via the road network. The total power of each node ζ consists of a distinct time-varying load $P_\zeta^{\text{load}}(t)$ and charging station power $P_\zeta(t)$. The power line connecting the node to the grid is designed to have adequate capacity to support its peak loads without EV charging, $\max P_\zeta^{\text{load}}(t) < \overline{P}_\zeta$, but the addition of large power consumption of the charging stations

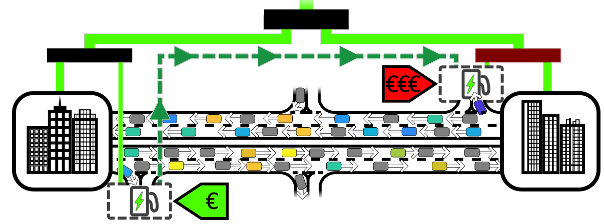

Fig. 1: Sketch of the studied system. EVs circulate between two urban nodes together with non-EVs. In this case, the load of the node on the right is too high, exceeding the line capacity. The controller reacts to this by increasing the charging price at that node and decreasing the charging price at the other one to induce a virtual power transmission and help the power grid.

may cause the total node power to exceed the power line capacity $\max P_\zeta^{\text{load}}(t) + P_\zeta(t) > \overline{P}_\zeta$ at some time t. The focus of this paper is on designing control laws for charging station prices and charging rates aimed at preventing such events, keeping $P_\zeta^{\text{load}}(t) + P_\zeta(t) \leq \overline{P}_\zeta$.

The EVs circulate between the two nodes, passing by both charging stations, and are able to charge at either of them. For each charging station ζ we define the baseline power $\hat{P}_\zeta(t)$ that it needs to supply to the EVs in order to keep the overall average SoC of the system ε_{avg} close to some reference level $\varepsilon^*_{\text{avg}}$. If a pair of charging stations is controlled so that the power consumption of the first one, ζ_-, is increased by some value, and the power consumption of the other, ζ_+, is decreased by the same value, this is equivalent to transmitting this power over a virtual power line. We denote the EVPL power transmission from charging station ζ_- to charging station ζ_+ by $P_{\text{EVPL}}^{\zeta_-,\zeta_+}(t)$, and define the reference powers that the pair of charging stations needs to follow

$$P^*_{\zeta_\pm}(t) = \hat{P}_{\zeta_\pm}(t) \mp P_{\text{EVPL}}^{\zeta_-,\zeta_+}(t).$$

The actual charging station powers $P_\zeta(t)$ are regulated to follow these reference powers by controlling their charging prices $u_\zeta(t)$ and charging rates $c_\zeta(t)$ as will be discussed in Section IV. In order to balance the power of the two nodes, we set the EVPL power transmission to

$$P_{\text{EVPL}}^{\zeta_1,\zeta_2}(t) = \frac{P_{\zeta_2}^{\text{load}}(t) - P_{\zeta_1}^{\text{load}}(t)}{2}, \tag{1}$$

equalizing the reference total power of the two nodes to

$$P_\zeta^{\text{load}}(t) + P^*_\zeta(t) = \hat{P}_\zeta(t) + \frac{P_{\zeta_2}^{\text{load}}(t) + P_{\zeta_1}^{\text{load}}(t)}{2}.$$

Note that thus defined EVPL shifts the power consumption spatially, from one charging station to the other, rather than temporally like the standard VPL. We may introduce the temporal dimension back into EVPL by deferring charging and allowing more overall SoC variation.

III. Modelling

We use a discretized Coupled Traffic, Energy, and Charging (CTEC) model [8] (see the cited paper for more details on its derivation), describing the dynamics of traffic and energy of the studied system, as the simulation ground-truth model. Here, we extend the model to explicitly handle a multi-class mixed traffic, with vehicle classes $\xi \in \Xi$, consisting of both EVs (of class $\xi \in \Xi_E$) and non-EVs ($\xi \in \Xi \setminus \Xi_E$). Then, we introduce some approximations to make the model tractable, and analyse the resulting simplified model which will be used for control design.

A. CTEC model

The full dynamics of the system are given by

$$\frac{\partial \rho_\zeta^\xi(x,t)}{\partial t} + \frac{\partial q_\zeta^\xi(x,t)}{\partial x} = 0, \qquad \xi \in \Xi, x \in [0, L_\zeta], \tag{2}$$

$$\frac{\partial \varepsilon_\zeta^\xi(x,t)}{\partial t} + v_\zeta(x,t)\frac{\partial \varepsilon_\zeta^\xi(x,t)}{\partial x} = \mathcal{D}^\xi(v_\zeta(x,t)), \; \xi \in \Xi_E, x \in [0, L_\zeta], \tag{3}$$

$$\frac{\partial \eta_\zeta(\varepsilon,t)}{\partial t} + c_\zeta(t)\frac{\partial \eta_\zeta(\varepsilon,t)}{\partial \varepsilon} = \dots$$
$$\dots \sum\nolimits_{\xi \in \Xi_E} \delta\left(\varepsilon - \varepsilon_\zeta^\xi(X_\zeta^-, t)\right) r_\zeta^\xi(t), \; \varepsilon \in [0,1], \tag{4}$$

for all links and charging stations $\zeta \in \mathcal{Z}$. With a slight abuse of notation we use the same symbol ζ to represent the charging station and the road link to which it is connected.

The state of road link ζ consists of the traffic density of all vehicle classes $\rho_\zeta^\xi(x,t)$, $\xi \in \Xi$, and SoC of the EVs $\varepsilon_\zeta^\xi(x,t)$, $\xi \in \Xi_E$, at position x at time t. We denote by $q_\zeta^\xi(x,t)$ the traffic flow of class ξ vehicles, $q_\zeta^\xi(x,t) = v_\zeta(x,t)\rho_\zeta^\xi(x,t)$, where the traffic speed $v_\zeta(x,t)$ depends on aggregate traffic density according to some nonincreasing function $\mathcal{V}(\rho)$,

$$v_\zeta(x,t) = \mathcal{V}(\rho_\zeta(x,t)), \quad \rho_\zeta(x,t) = \sum\nolimits_{\xi \in \Xi} \rho_\zeta^\xi(x,t),$$

also defining the fundamental diagram $Q(\rho) = \rho\mathcal{V}(\rho)$. The energy in EVs' batteries is transported along the road at the speed of the traffic $v_\zeta(x,t)$, and discharged according to some function $\mathcal{D}^\xi(v)$ depending on their speed.

The state of charging station is defined by the accumulation of EVs at different SoC $\eta_\zeta(\varepsilon,t)$. In this work we assume that all EVs at a single charging station are charged at the same rate $c_\zeta(t)$, in the range of $0 \leq \underline{C} \leq c_\zeta(t) \leq \overline{C}$, and that the EVs leave as soon as they are fully charged, yielding exiting flow

$$\mu_\zeta(t) = c_\zeta(t)\eta_\zeta(1,t).$$

This yields the charging station power $P_\zeta(t)$ of

$$P_\zeta(t) = Ec_\zeta(t)\int_0^1 \eta_\zeta(\varepsilon,t)\mathrm{d}\varepsilon = Ec_\zeta(t)\eta_\zeta^{\text{tot}}(t),$$

where E is the average EV battery capacity, and we denote by $\eta_\zeta^{\text{tot}}(t)$ the total number of EVs at charging station ζ. Finally, the inhomogeneous part of (4) models the flow of all classes of EVs entering the charging station from the road, with SoC $\varepsilon_\zeta^\xi(X_\zeta^-, t)$. Function $\delta(\varepsilon)$ is taken to be a finite approximation of the Dirac delta function with support $[-L_\delta, L_\delta]$, where $L_\delta \approx 0^+$, $\delta(\varepsilon) = \frac{1}{2L_\delta}, |\varepsilon| \leq L_\delta$.

We connect the road traffic states with the charging stations' states and the external world by ramp flows, through defining internal boundary conditions

$$q_\zeta^\xi(X_\zeta^+,t) = q_\zeta^\xi(X_\zeta^-,t) - r_\zeta^\xi(t) + \mu_\zeta^\xi(t), \qquad \xi \in \Xi_E, \tag{5}$$

$$q_\zeta^\xi(X_\zeta^+,t)\varepsilon_\zeta^\xi(X_\zeta^+,t) = \left(q_\zeta^\xi(X_\zeta^-,t) - r_\zeta^\xi(t)\right)\varepsilon_\zeta^\xi(X_\zeta^-,t) + \mu_\zeta^\xi(t), \; \xi \in \Xi_E, \tag{6}$$

$$q_\zeta^\xi(X_\zeta^{\text{ext},+},t) = q_\zeta^\xi(X_\zeta^{\text{ext},-},t) - r_\zeta^{\text{ext},\xi}(t) + \mu_\zeta^{\text{ext},\xi}(t), \xi \in \Xi \setminus \Xi_E, \tag{7}$$

with (5) defining the flow of EVs entering (r_ζ^ξ) and exiting (μ_ζ^ξ) charging station ζ at position X_ζ, (6) defining the flow of energy carried in their batteries, and (7) defining the flow of non-EVs leaving the road via an off-ramp (r_ζ^ξ) and entering the road via an on-ramp (μ_ζ^ξ) at position X_ζ^{ext}. For the non-EVs, these flows are given by constant splitting ratios towards the off-ramp $\beta_\zeta^{\text{ext},\xi}$,

$$r_\zeta^{\text{ext},\xi}(t) = \beta_\zeta^{\text{ext},\xi} q_\zeta^\xi(X_\zeta^{\text{ext},-},t), \quad \xi \in \Xi \setminus \Xi_E,$$

and by externally defined on-ramp flow $\mu_\zeta^{\text{ext},\xi}(t)$. For the EVs, the flow leaving the road and entering charging station ζ at position X_ζ is given by

$$r_\zeta^\xi(t) = \beta\left(\varepsilon_\zeta^\xi(X_\zeta,t), u_\zeta(t)\right) q_\zeta^\xi(X_\zeta,t), \quad \xi \in \Xi_E, \tag{8}$$

where $u_\zeta(t)$ is the charging price, and function $\beta(\varepsilon,u)$ describes the splitting ratio of EVs towards the charging station depending on their SoC and the charging price,

$$\beta(\varepsilon,u)=1-\left(1+e^{-\frac{\varepsilon-(U_0+U_1u)}{\sigma}}\right)^{-1}.$$

Here $U_0>0$ and $U_1<0$ are parameters defining the SoC U_0+U_1u at which 50% EVs enter the charging station (as the EVs' SoC decreases, a larger portion enters the charging station), and σ parametrizes the spread of the SoC of EVs entering around this value.

Finally, we assume that the non-EVs $\xi\in\Xi\setminus\Xi_E$ continue circulating after reaching the end of the road link, $q^{\xi}_{\zeta}(0,t)=q^{\xi}_{\overleftarrow{\zeta}}(L_{\overleftarrow{\zeta}},t)$, until they leave the road via an off-ramp at position X^{ext}_{ζ}. Here, we denote by $\overleftarrow{\zeta}$ the road link that is upstream of road link ζ, i.e. vehicles arrive from the downstream end of the link $\overleftarrow{\zeta}$, and then continue on link ζ. The EVs $\xi\in\Xi_E$ instead spend some time at the node and return to the road after an average delay of $\tau_{\bar{\zeta}}$,

$$q^{\xi}_{\zeta}(0,t)=q^{\xi}_{\overleftarrow{\zeta}}(L_{\overleftarrow{\zeta}},t-\tau_{\bar{\zeta}}),$$

during which they are kept in a virtual charging station $\bar{\zeta}$,

$$\frac{\partial\bar{\eta}^{\xi}_{\bar{\zeta}}(\varepsilon,t)}{\partial t}=\delta\Big(\varepsilon-\varepsilon^{\xi}_{\overleftarrow{\zeta}}(L_{\overleftarrow{\zeta}},t)\Big)q^{\xi}_{\overleftarrow{\zeta}}(L_{\overleftarrow{\zeta}},t)-\delta\Big(\varepsilon-\varepsilon^{\xi}_{\zeta}(0,t)\Big)q^{\xi}_{\zeta}(0,t),$$

with $\varepsilon^{\xi}_{\zeta}(0,t)$ taking random values in set $\mathcal{E}_{\bar{\eta}}(t)$,

$$\mathcal{E}_{\bar{\eta}}(t)=\left\{e\in[0,1]\,\middle|\,\int_0^1\delta(\varepsilon-e)\,\bar{\eta}^{\xi}_{\bar{\zeta}}(\varepsilon,t)\mathrm{d}\varepsilon>0\right\},$$

ensuring $(\forall t\in\mathbb{R}_{\geq 0},\varepsilon\in[0,1]),\bar{\eta}^{\xi}_{\bar{\zeta}}(\varepsilon,t)\geq 0$.

B. Model simplification and analysis

In order to make the analysis and control design tractable, the CTEC model needs to be simplified, through appropriate approximations. We adopt a simplified charging station model similar to the one in [8] and extend the analysis given therein to specify what range of charging station powers may be achieved. Since we consider a single class of EVs ξ and a single charging station ζ, we omit writing these identifiers in the remainder of this Section wherever unabmiguous.

Since the outer control loop regulates the average SoC in the whole system $\varepsilon_{\text{avg}}(t)$ to some reference value $\varepsilon^*_{\text{avg}}$, we assume that the SoC of the EVs entering any charging station will be approximately constant $\varepsilon\approx\varepsilon^{\text{in}}$. Since the EVs leave the charging station with SoC $\varepsilon=1$, we may split the interval $[\varepsilon^{\text{in}},1]$ in which $\eta(\varepsilon,t)$ is nonzero into equal parts, $[\varepsilon^{\text{in}},\tilde{\varepsilon}]$ and $[\tilde{\varepsilon},1]$, with $\tilde{\varepsilon}=\frac{1+\varepsilon^{\text{in}}}{2}$, and study the second-order approximation of $\eta(\varepsilon,t)$, with states $\eta^{\text{lo}}(t)$ and $\eta^{\text{hi}}(t)$

$$\eta^{\text{lo}}(t)=\int_0^{\tilde{\varepsilon}}\eta(\varepsilon,t)\mathrm{d}\varepsilon,\quad \eta^{\text{hi}}(t)=\int_{\tilde{\varepsilon}}^1\eta(\varepsilon,t)\mathrm{d}\varepsilon.$$

Charging station dynamics (4) then simplify to

$$\dot{\eta}^{\text{lo}}(t)=r(t)-\frac{c(t)}{L^{\varepsilon}}\eta^{\text{lo}}(t),$$

$$\dot{\eta}^{\text{hi}}(t)=\frac{c(t)}{L^{\varepsilon}}\eta^{\text{lo}}(t)-\frac{c(t)}{L^{\varepsilon}}\eta^{\text{hi}}(t),$$

where $L^{\varepsilon}=1-\tilde{\varepsilon}=\tilde{\varepsilon}-\varepsilon^{\text{in}}$. For constant r and c, we have the equilibrium of $\eta^{\text{lo}}(t)\to\eta^{\text{lo}}_{\text{eq}}=\frac{rL^{\varepsilon}}{c}$ and $\eta^{\text{hi}}(t)\to\eta^{\text{hi}}_{\text{eq}}=\frac{rL^{\varepsilon}}{c}$, yielding total number of EVs $\eta^{\text{tot}}(t)\to\eta^{\text{tot}}_{\text{eq}}=\frac{2rL^{\varepsilon}}{c}$, and equilibrium charging station power $P(t)\to P_{\text{eq}}=2ErL^{\varepsilon}$, depending only on the flow of EVs entering the charging station r, and not on the charging rate c.

This indicates that in order to be able to make $P(t)$ track some reference power $P^*(t)$ over an infinite time horizon, we need to control the EV inflow $r(t)$. However, assuming

$$\frac{P^*_{\zeta}(t)}{\overline{C}}\leq\eta^{\text{tot}}_{\zeta}(t)\leq\frac{P^*_{\zeta}(t)}{\underline{C}},\tag{9}$$

we can force $P(t)=P^*(t)$ over a finite time horizon, by controlling the charging rate

$$c(t)=c^*_{\zeta}(t)=\max\left\{\underline{C},\min\left\{\overline{C},\frac{P^*(t)}{\eta^{\text{tot}}(t)}\right\}\right\}.\tag{10}$$

This case can be analysed by adopting a state transformation

$$\dot{\eta}^{\text{tot}}(t)=r(t)\left(1-\frac{2P^*(t)}{P_{\text{eq}}(1+\gamma(t))}\right),\tag{11}$$

$$\dot{\gamma}(t)=\frac{r(t)}{\eta^{\text{tot}}(t)}\left(1+\gamma(t)-2\frac{P^*(t)}{P_{\text{eq}}}\gamma^2(t)\right),$$

where $\gamma(t)=\frac{\eta^{\text{lo}}(t)}{\eta^{\text{hi}}(t)}$, assuming $\eta^{\text{hi}}(t)>0$.

Finally, we briefly discuss simplifying the model of the flow of EVs entering the charging station $r(t)$. In this context, the full road dynamics (2)–(3) can be reduced into a time-delay system with state-dependant time delay originating from the travel time, the charging time, and the node dwell time. This reformulation makes the analysis intractable, so we instead resort to linearizing $r(t)$, whose exact form is given by (8), with respect to $u(t)$,

$$r(t)\approx R(t)+S(t)u(t),\tag{12}$$

where $R(t)>0$ and $S(t)<0$ are unknown, potentially time-varying parameters, and deal with this uncertainty through feedback control.

One useful approximate aggregate quantity is the average total battery discharge power,

$$P_{\mathcal{D}}\approx EL^x_{\text{tot}}\rho^E_{\text{avg}}\mathcal{D}(v_{\text{avg}})<0,$$

where L^x_{tot} is the total length of the road, ρ^E_{avg} the average density of EVs, and v_{avg} the average speed of all vehicles on it. Since this quantity is easier to estimate than the actual total battery discharge power, it allows for a simple approximation of the overall average SoC dynamics,

$$\dot{\varepsilon}_{\text{avg}}(t)\approx\frac{P_{\mathcal{D}}+\sum_{\zeta\in\mathcal{Z}}P_{\zeta}(t)}{N_E E},\tag{13}$$

where N_E is the total number of EVs in the system, both on the road and at the charging stations or at urban nodes. It is clear that for $\varepsilon_{\text{avg}}(t)$ not to diverge from its reference value $\varepsilon^*_{\text{avg}}$, the total power of all charging stations needs to equal the total battery discharge power. However, this power need not be spread equally among the charging stations, which we use for defining and implementing EVPLs.

IV. Control

As discussed in Section II, the overall control objective is to ensure that the charging station powers follow their references, including the EVPL power transmission, while keeping the SoC of the system adequate. The EVPL power transmission will in turn designed such that all node powers would be balanced, in order to avoid violating their capacity constraints. The control action can be split into three layers according to their time scale:

1) Baseline power adaptation,
2) Nominal power reference tracking, and
3) Charging rate control and compensation.

In order to make the control setup more realistic, we change the charging station prices at discrete instants, with a time step of $T_{\mathrm{step}} = 15$ min, which should allow the drivers enough time to react to the pricing signal communicated to them. The charging rates $c_\zeta(t)$ are controlled continuously.

1) Baseline power adaptation: The slowest control layer is tasked with finding the baseline power of the charging stations $\hat{P}_\zeta(t)$ that keeps the average overall SoC of the system $\varepsilon_{\mathrm{avg}}(t)$ close to its reference value $\varepsilon^*_{\mathrm{avg}}$. Due to the symmetry of the system studied in this work, we assign the same baseline power to both charging stations. We set the baseline power as the output of a simple PI controller, The

$$\hat{P}_\zeta(t) = K^\varepsilon_{\mathrm{p}} e^\varepsilon_{\mathrm{p}}(t) + K^\varepsilon_{\mathrm{i}} e^\varepsilon_{\mathrm{i}}(t), \tag{14}$$

where the error signal and its integral are

$$e^\varepsilon_{\mathrm{p}}(t) = \varepsilon^*_{\mathrm{avg}} - \varepsilon_{\mathrm{avg}}(t), \quad e^\varepsilon_{\mathrm{i}}(t+T) = e^\varepsilon_{\mathrm{i}}(t) + T_{\mathrm{step}} e^\varepsilon_{\mathrm{p}}(t).$$

The integral error is initialized at time t_0, when we start controlling the system, to

$$e^\varepsilon_{\mathrm{i}}(t_0) = \frac{P_{\mathcal{D}}}{2K^\varepsilon_{\mathrm{i}}},$$

according to the approximate average error dynamics (13).

2) Nominal power reference tracking: The reference power of each charging station $P^*_\zeta(t)$ is given as the sum of its baseline power $\hat{P}_\zeta(t)$ (14) and its EVPL power transmission reference $P^{\zeta,\bar{\zeta}}_{\mathrm{EVPL}}(t)$,

$$P^*_\zeta(t) = \hat{P}_\zeta(t) + P^{\zeta,\bar{\zeta}}_{\mathrm{EVPL}}(t),$$

where we denote by $\bar{\zeta}$ the *other* charging station, and $P^{\zeta,\bar{\zeta}}_{\mathrm{EVPL}}(t) = -P^{\bar{\zeta},\zeta}_{\mathrm{EVPL}}(t)$. The second control layer ensures that the nominal power of a charging station, defined as the power under some nominal charging rate C_{nom}, tracks this reference value, by controlling the charging price $u^P_\zeta(t)$. This can be achieved by another PI controller,

$$u^P_\zeta(t) = K^P_{\mathrm{p}} e^P_{\mathrm{p}}(t) + K^P_{\mathrm{i}} e^P_{\mathrm{i}}(t)$$

with error and error integral defined as

$$e^P_{\mathrm{p}}(t) = P^*_\zeta(t) - E C_{\mathrm{nom}} \eta^{\mathrm{tot}}_\zeta(t), e^P_{\mathrm{i}}(t+T) = e^P_{\mathrm{i}}(t) + T_{\mathrm{step}} e^P_{\mathrm{p}}(t),$$

and the integral error initialized so that $u^P_\zeta(t_0)$ starts from some nominal price u_{nom},

$$e^P_{\mathrm{i}}(t_0) = \frac{u_{\mathrm{nom}}}{K^P_{\mathrm{i}}}.$$

3) Charging rate control and compensation: Finally, while the second control layer brings the nominal charging station power $E C_{\mathrm{nom}} \eta^{\mathrm{tot}}_\zeta(t)$ close to its reference value $P^*_\zeta(t)$, due to the long time step and strong nonlinearity of the system, there are severe limitations on its tracking performance. However, since we assume that the charging rates can be controlled instantaneously, if the total number of vehicles at the charging station is within (9) we achieve $P_\zeta(t) = P^*_\zeta(t)$ by setting the charging rate to (10). As the analysis in Section III-B shows, if the inflow to the charging station is kept constant and this charging rate is applied, $\eta^{\mathrm{tot}}_\zeta(t)$ leaves the range (9) within some time T_{lim}, making it impossible to keep $P_\zeta(t) = P^*_\zeta(t)$. Therefore, we offset the effect of controlling the charging rate by adding a compensation term $u^{\mathrm{c}}_\zeta(t)$ to the charging price,

$$u_\zeta(t) = u^P_\zeta(t) + u^{\mathrm{c}}_\zeta(t).$$

The compensation term is calculated from the condition that the simplified model (11) with $\gamma_\zeta(t) \approx 1$ and $r_\zeta(t)$ given by (12) with constant EV inflow linearization parameters $\hat{R}$ and $\hat{S}$ fitted from simulation data,

$$\dot{\eta}^{\mathrm{tot}}_\zeta(t) = \hat{R} + \hat{S} u_\zeta(t) - \frac{c_\zeta(t) \eta^{\mathrm{tot}}_\zeta(t)}{2L^\varepsilon}$$

results in the same $\eta^{\mathrm{tot}}_\zeta(t+T)$ for the same $\eta^{\mathrm{tot}}_\zeta(t)$ when $c_\zeta(t) = C_{\mathrm{nom}}$ and $u_\zeta(t) = u^P_\zeta(t)$, and when $c_\zeta(t) = c^*_\zeta(t)$ and $u_\zeta(t) = u^P_\zeta(t) + u^{\mathrm{c}}_\zeta(t)$, yielding

$$u^{\mathrm{c}}_\zeta(t) = \frac{1}{S}\left(\frac{P^*_\zeta(t)}{2L_\varepsilon E} - \alpha \eta^{\mathrm{tot}}_\zeta(t) - \left(1 - \frac{2L_\varepsilon \alpha}{C_{\mathrm{nom}}}\right)\left(\hat{R} + \hat{S} u^P_\zeta(t)\right)\right),$$

with $\alpha = \frac{1}{T_{\mathrm{step}}}\left(1 - e^{-\frac{C_{\mathrm{nom}}}{2L_\varepsilon} T_{\mathrm{step}}}\right)$.

V. SIMULATION RESULTS

Finally, we test the proposed EVPL framework and the control law that achieves it in simulations. The simulation setup is shown in Figure 1, and its main parameters, including the controller parameters, are given in Table I. It consists of two urban nodes connected by road of length $L^x = 50$ km. Each simulation run is $t_{\mathrm{end}} = 24$ h long, and the average dwell time of EVs at the two nodes is set to $\tau_{\bar{\zeta}} = 30$ min. At the exit from each node, there is a charging station connected to the same port of the power grid. Close to the middle of the road, there is an on-off-ramp pair, where a portion of $\beta^{\mathrm{ext}}_\zeta = 0.25$ non-EVs leave the road, and the on-ramp flow of non-EVs is uniformly distributed, $r^{\mathrm{ext}}_\zeta(t) \sim \mathcal{U}_{[0.11 Q_{\max}, 0.22 Q_{\max}]}$ where $Q_{\max}$ denotes the road capacity. All EVs remain in the system, and do not interact with these on- and off-ramps.

The simulation is initialized with uniformly distributed initial traffic density $\rho_\zeta(x,0) \sim \mathcal{U}_{[0.7\rho_{\mathrm{cr}}, 1.2\rho_{\mathrm{cr}}]}$, where ρ_{cr} is the critical density, and empty charging stations. The initial share of EVs at each point is $\rho^{\xi_E}_\zeta(x,0)/\rho_\zeta(x,0) \sim \mathcal{U}_{[0,1]}$, and their initial SoC is $\varepsilon^{\xi_E}_\zeta(x,0) \sim \mathcal{U}_{[0.45,0.55]}$. The dynamics of the roads are defined by the average speed function

$$\mathcal{V}(\rho) = V e^{-\frac{1}{2}\left(\frac{\rho}{\rho_{\mathrm{cr}}}\right)^2},$$

and a polynomial battery discharge function

$$\mathcal{D}(v) = -k^{\mathcal{D}}_0 - k^{\mathcal{D}}_1 v - k^{\mathcal{D}}_2 v^2.$$

The two nodes have the same power capacity $\overline{P}_\zeta = 1.5$ MW, and their load profiles are taken to be perturbed sinusoids with different frequencies

$$P^{\mathrm{load}}_\zeta(t) = p^{\mathrm{var}}_\zeta(t)\left(b^{\mathrm{load}}_\zeta - a^{\mathrm{load}}_\zeta \cos(\omega_\zeta t)\right),$$

where $p^{\mathrm{var}}_\zeta(t) \sim \mathcal{U}_{[0.95,1.05]}$ is the multiplicative noise modelling load variation. We set $\omega_{\zeta_1} = \frac{2\pi}{24\mathrm{h}}$ and $\omega_{\zeta_2} = 2\omega_{\zeta_1}$, i.e. the loads of nodes ζ_1 and ζ_2 have periods of 24 h and 12 h, respectively. The bias and amplitude parameters are

Symbol	Value	Unit	Symbol	Value	Unit
L^x	50	km	$\hat{R}$	0.5	1
T_{step}	15	min	$\hat{S}$	-0.05	1
E	0.06	MWh	$K^\varepsilon_{\mathrm{p}}$	10	MW
$\underline{C}$	0.83	1/h	$K^\varepsilon_{\mathrm{i}}$	$0.8333 \cdot 10^{-9}$	MW/h
C_{nom}	1.25	1/h	K^P_{p}	1	1/MW
$\overline{C}_\zeta$	1.67	1/h	K^P_{i}	$4.1667 \cdot 10^{-6}$	1/MWh
U_0	0.8	1	V	100	km/h
U_1	-0.5	1	ρ_{cr}	15	veh/km
σ	0.05	1	$P_{\mathcal{D}}$	1	MW
$\varepsilon^{\mathrm{in}}$	0.475	1	$\bar{P}$	1.5	MW

TABLE I: Simulation parameters and their values.

set to $b_{\zeta_1}^{\mathrm{load}} = 0.65$ MW, $a_{\zeta_1}^{\mathrm{load}} = 0.4$ MW, $b_{\zeta_2}^{\mathrm{load}} = 0.8$ MW, and $a_{\zeta_2}^{\mathrm{load}} = 0.3$ MW, and the average total battery discharge power is calculated to be $P_{\mathcal{D}} \approx 1$ MW, which means that the power of the two charging stations will be close to 0.5 MW on average. It can be seen from the parameters that unless the charging stations are controlled, the total power of both nodes will exceed the capacity at their peak load times, but since these peak load times do not coincide, the control works to avoid this by setting the EVPL power transmission reference (1) to balance their powers.

After a warm-up period of $t_{\mathrm{w}} = 1$ h, when the charging prices and charging rates are kept at their nominal values u_{nom} and C_{nom}, respectively, the controllers are initialized and start tracking the references. We compare three cases of control, differing by what control inputs are used:

1) Price only, $u_\zeta(t) = u_\zeta^P(t)$, $c_\zeta(t) = C_{\mathrm{nom}}$
2) Both price and charging rate, without compensation, $u_\zeta(t) = u_\zeta^P(t)$, $c_\zeta(t)$ given by (10), and
3) Both price and charging rate, with compensation, $u_\zeta(t) = u_\zeta^P(t) + u_\zeta^c(t)$, $c_\zeta(t)$ given by (10).

We evaluate the performance of the proposed control laws by comparing two metrics: mean square tracking error

$$J_{\mathrm{MSE}} = \sum_{\zeta \in \mathcal{Z}} \frac{1}{t_{\mathrm{end}} - t_{\mathrm{w}}} \int_{t_{\mathrm{w}}}^{t_{\mathrm{end}}} \big(P_\zeta(t) - P_\zeta^*(t)\big)^2 \mathrm{d}t,$$

and total capacity violation

$$J_{\mathrm{cap}} = \sum_{\zeta \in \mathcal{Z}} \int_{t_{\mathrm{w}}}^{t_{\mathrm{end}}} \max\left\{0, P_\zeta^{\mathrm{load}}(t) + P_\zeta(t) - \overline{P}_\zeta\right\} \mathrm{d}t.$$

The mean values of these metrics for 100 simulation runs are shown in Table II. It can be seen that all the proposed control laws significantly reduce capacity violations compared to the uncontrolled case when $u_\zeta(t) = u_{\mathrm{nom}}$, $c_\zeta(t) = C_{\mathrm{nom}}$. The control laws with $c_\zeta(t) = c_\zeta^*(t)$ achieve better performance than the one with $c_\zeta(t) = C_{\mathrm{nom}}$, both in terms of reference tracking and capacity violations, especially when the influence of charging rate control is compensated.

In order to further explain the operation of the proposed control laws, details from one characteristic simulation run are shown in Figures 2–6. As shown in Figure 2, all control laws slowly bring $\varepsilon_{\mathrm{avg}}(t)$ to its reference value $\varepsilon_{\mathrm{avg}}^* = 0.5$, whereas in the uncontrolled case it settles at a lower value. The resulting total node powers $P_\zeta^{\mathrm{load}}(t) + P_\zeta(t)$ are shown in Figure 3. In the uncontrolled case, shown in Figure 3 (0), the power of both nodes exceeds the capacity at different times, with $J_{\mathrm{cap}}^0 = 1.0490$. All control laws significantly reduce the capacity violations, with $J_{\mathrm{cap}}^1 = 0.2187$, $J_{\mathrm{cap}}^2 = 0.0805$, and $J_{\mathrm{cap}}^3 = 0.0518$, with particularly good results when charging rate control $c_\zeta(t) = c_\zeta^*(t)$ is used. The power reference tracking performance of the three control cases can be seen in Figure 4. The control law with $c_\zeta(t) = C_{\mathrm{nom}}$ achieves

	$u_{\mathrm{nom}}, C_{\mathrm{nom}}$	$u_\zeta^P, C_{\mathrm{nom}}$	u_ζ^P, c_ζ^*	$u_\zeta^P + u_\zeta^c, c_\zeta^*$
J_{MSE} [MW^2]	–	0.0160	0.0122	0.0064
J_{cap} [MWh]	0.6993	0.1029	0.0429	0.0221

TABLE II: Average performance of the three evaluated control laws over 100 simulation runs.

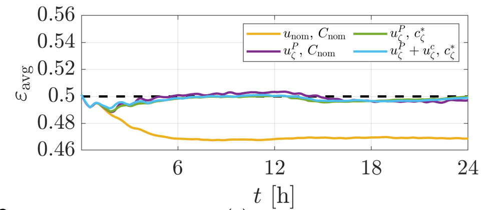

Fig. 2: Average SoC $\varepsilon_{\mathrm{avg}}(t)$ over the course of an example simulation run for the uncontrolled and the three controlled cases.

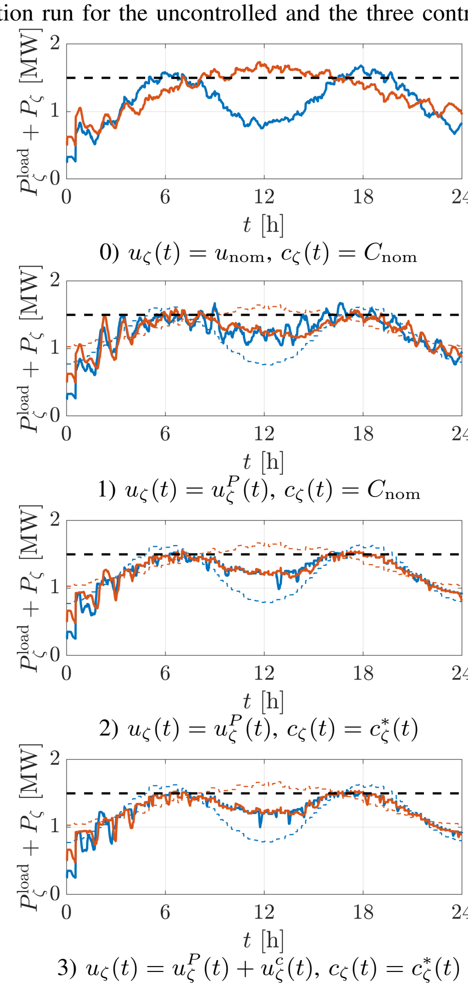

Fig. 3: Node powers in the uncontrolled and controlled cases. Dashed lines show the reference node powers $P_\zeta^{\mathrm{load}}(t) + \hat{P}_\zeta(t)$ without the contribution of EVPL.

visibly worse tracking, with $J_{\mathrm{MSE}}^1 = 0.0217$, compared to the other two control laws with $J_{\mathrm{MSE}}^2 = 0.0094$ and $J_{\mathrm{MSE}}^3 = 0.0076$. Improved tracking performance does result in a more oscillatory price signal $u_\zeta(t)$, as can be seen in Figure 5. Finally, the achieved EVPL power transmission is shown in Figure 6, with almost perfect tracking after the initial transient period in case of control using $u_\zeta(t) = u_\zeta^P(t) + u_\zeta^c(t)$ and $c_\zeta(t) = c_\zeta^*(t)$.

VI. Conclusions

In this work we propose and evaluate a grid management strategy, that we coin *EV Virtual Power Lines*, relying on controlling the charging stations in a way that shifts power consumption from one point in the grid to another, without disrupting the EV fleet operation by postponing its charging

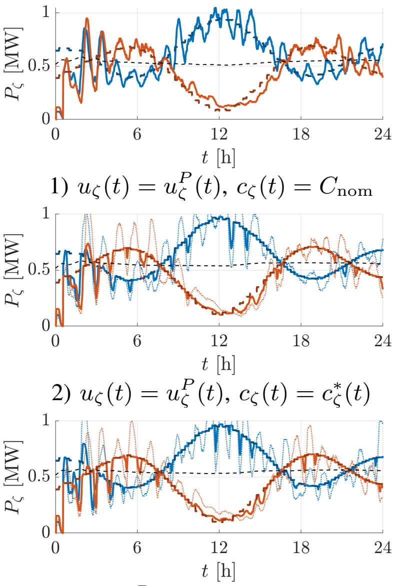

1) $u_\varsigma(t) = u^P_\varsigma(t)$, $c_\varsigma(t) = C_{\mathrm{nom}}$

2) $u_\varsigma(t) = u^P_\varsigma(t)$, $c_\varsigma(t) = c^*_\varsigma(t)$

3) $u_\varsigma(t) = u^P_\varsigma(t) + u^c_\varsigma(t)$, $c_\varsigma(t) = c^*_\varsigma(t)$

Fig. 4: Charging station powers $P_\varsigma(t)$. Thick dashed lines show the reference powers $P^*_\varsigma(t)$, thin black dashed line the baseline powers $\hat{P}_\varsigma(t)$, and thin dotted line the nominal powers $C_{\mathrm{nom}}\eta^{\mathrm{tot}}_\varsigma(t)$.

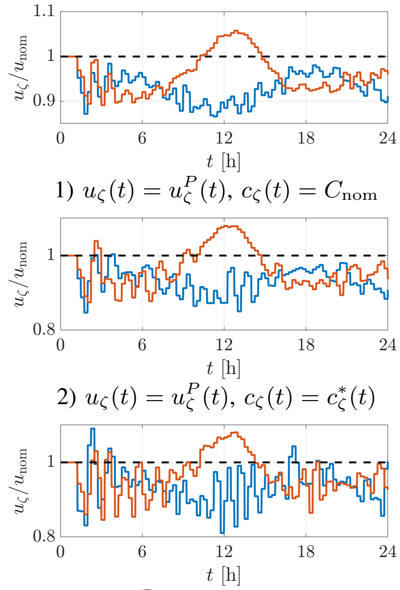

1) $u_\varsigma(t) = u^P_\varsigma(t)$, $c_\varsigma(t) = C_{\mathrm{nom}}$

2) $u_\varsigma(t) = u^P_\varsigma(t)$, $c_\varsigma(t) = c^*_\varsigma(t)$

3) $u_\varsigma(t) = u^P_\varsigma(t) + u^c_\varsigma(t)$, $c_\varsigma(t) = c^*_\varsigma(t)$

Fig. 5: Relative charging prices of the two charging stations $u_\varsigma(t)/u_{\mathrm{nom}}$.

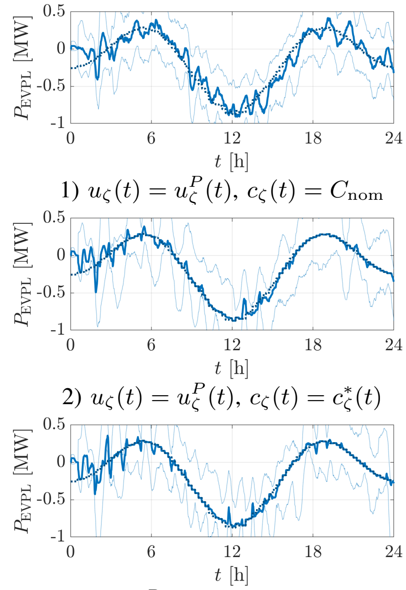

1) $u_\varsigma(t) = u^P_\varsigma(t)$, $c_\varsigma(t) = C_{\mathrm{nom}}$

2) $u_\varsigma(t) = u^P_\varsigma(t)$, $c_\varsigma(t) = c^*_\varsigma(t)$

3) $u_\varsigma(t) = u^P_\varsigma(t) + u^c_\varsigma(t)$, $c_\varsigma(t) = c^*_\varsigma(t)$

Fig. 6: Achieved EVPL power transmission $P_{\mathrm{EVPL}}(t)$. Thick dotted line shows its reference and thin dotted lines its current minimum and maximum achievable values due to $\underline{C} \leq c_\varsigma(t) \leq \overline{C}$.

times. Control laws that achieve this goal were presented, compared, and shown to be able to control the charging station power in a way that decongests the power grid.

This work focuses on providing a proof of concept on the simplest possible setup. In the future, we seek to extend these results and apply them on a more realistic urban electromobility case, explicitly identifying which electromobility parameters (e.g. total EV traffic flow profiles in space and time) determine how much EVPL power transmission can be achieved between different geographical points. Additionally, here we focused explicitly on shifting the power consumption in space, without changing the time profile of the total charging power. This approach may prove to be overly conservative, since some drift of SoC can be allowed in case the grid cannot be decongested simply by shifting the charging power in space. Finally, practical aspects such as the explicit consideration of the distribution system topology, as well as EV drivers' reaction to the incentives, remain to be considered in more detail.

References

[1] J. Zhao, C. Wang, B. Zhao, F. Lin, Q. Zhou, and Y. Wang, "A review of active management for distribution networks: Current status and future development trends," *Electric Power Components and Systems*, vol. 42, no. 3-4, pp. 280–293, 2014.

[2] D. Pudjianto, C. Ramsay, and G. Strbac, "Virtual power plant and system integration of distributed energy resources," *IET Renewable power generation*, vol. 1, no. 1, pp. 10–16, 2007.

[3] C. Binding, D. Gantenbein, B. Jansen, *et al.*, "Electric vehicle fleet integration in the danish EDISON project – a virtual power plant on the island of Bornholm," in *IEEE PES general meeting*, IEEE, 2010, pp. 1–8.

[4] L. Zhou, F. Li, C. Gu, Z. Hu, and S. Le Blond, "Cost/benefit assessment of a smart distribution system with intelligent electric vehicle charging," *IEEE Transactions on Smart Grid*, vol. 5, no. 2, pp. 839–847, 2013.

[5] R. Henry and D. Ernst, "Gym-ANM: Reinforcement learning environments for active network management tasks in electricity distribution systems," *Energy and AI*, vol. 5, p. 100 092, 2021.

[6] M. Čičić, C. Vivas, C. Canudas-de-Wit, and F. R. Rubio, "Optimal renewable energy curtailment minimization control using a combined electromobility and grid model," in *IFAC World Congress*, 2023.

[7] H. Nakano, I. Nawata, S. Inagaki, *et al.*, "Aggregation of V2H systems to participate in regulation market," *IEEE Transactions on Automation Science and Engineering*, vol. 18, no. 2, pp. 668–680, 2020.

[8] M. Čičić, G. Gasnier, and C. Canudas-de-Wit, "Electric vehicle charging station pricing control under balancing reserve capacity commitments," in *IEEE 62nd Conference on Decision and Control (CDC)*, 2023.

[9] M. T. Kahlen, W. Ketter, and J. van Dalen, "Electric vehicle virtual power plant dilemma: Grid balancing versus customer mobility," *Production and Operations Management*, vol. 27, no. 11, pp. 2054–2070, 2018.

[10] G. Wenzel, M. Negrete-Pincetic, D. E. Olivares, J. MacDonald, and D. S. Callaway, "Real-time charging strategies for an electric vehicle aggregator to provide ancillary services," *IEEE Transactions on Smart Grid*, vol. 9, no. 5, pp. 5141–5151, 2017.

[11] F. Paparella, T. Hofman, and M. Salazar, "Joint optimization of number of vehicles, battery capacity and operations of an electric autonomous mobility-on-demand fleet," in *2022 IEEE 61st Conference on Decision and Control (CDC)*, IEEE, 2022, pp. 6284–6291.

[12] IRENA, "Virtual power lines," International Renewable Energy Agency Abu Dhabi, Tech. Rep., 2020.